Structural and Functional Properties of Full-Length and Truncated Human Proapolipoprotein AI Expressed in *Escherichia coli*†

Louise E. Pyle,‡ William H. Sawyer,§ Yoko Fujiwara,‡ Alana Mitchell,‡ and Noel H. Fidge*,‡

Baker Medical Research Institute, Commercial Road, Prahran, 3181, Australia, and Department of Biochemistry, University of Melbourne, Parkville, 3052, Australia

Received April 15, 1996; Revised Manuscript Received July 8, 1996⊗

ABSTRACT: Utilizing the *Escherichia coli*/pGex vector expression system incorporating a thrombin cleavage site, full-length (residues −6−243) and truncated forms of proapolipoprotein AI (proapoAI), terminating at amino acid residues 222, 210, 150, and 135, were purified to levels of at least 5 mg/L, after thrombin cleavage. Assessed by circular dichroism, the helical contents of L-α-dimyristoylphosphatidylcholine-associated forms of human plasma-derived apolipoprotein AI (apoAI) and recombinant proapoAI were comparable, being 69% and 65%, respectively. Circular dichroism measurements of the lipid-associated complexes of the truncated forms showed that between the sequence of residues 150−222 no additional helicity was gained until the carboxyl-terminal sequence was present in the molecule, indicating that the carboxyl terminus of the protein is required for the formation of helix within this central region. While tryptophan residues were more than 86% accessible, as assessed by iodide quenching, in the two truncated forms, proapoAI$_{-6-135}$ and proapoAI$_{-6-150}$, for both free and complexed protein, this figure fell to about 50% for full-length recombinant proapoAI, further indicating the influence of the carboxyl terminus on the structure of the whole protein. While cross-linking human plasma apoAI in solution with dithiobis-(succinimidyl propionate) revealed high molecular weight oligomers by sodium dodecyl sulfate−polyacrylamide gel electrophoresis, recombinant proapoAI did not strongly form complexes larger than trimers. None of the truncated proapoAI molecules formed oligomers larger than trimers. The shortest form, proapoAI$_{-6-135}$, only dimerized. Initial results from lecithin:cholesterol acyltransferase activation (apoAI peptide concentration 0.2 μM) indicated that truncation of the 21 carboxy-terminal amino acids resulted in a drop of approximately 53% in activation and 33 residues a drop of 67% relative to the full-length protein. Overall these results indicate the important influence of the carboxyl terminus on the structure of apoAI.

Apolipoprotein AI (apoAI),[1] the principal protein moiety of high-density lipoprotein (HDL), plays an influential role in the process of reverse cholesterol transport (Fielding & Fielding, 1995; Barter, 1993) and is the main activator of lecithin:cholesterol acyltransferase (LCAT), an enzyme responsible for esterification of cholesterol in plasma (Fielding et al., 1972; Jonas, 1987). Elevated HDL levels and a reduced risk of developing atherosclerosis are paralleled by a corresponding relationship between plasma apoAI levels and risk for cardiovascular disease. Some studies suggest that plasma apoAI is in fact a better predictor of risk than (total) cholesterol or apolipoprotein B concentrations (Maciejko et al., 1983). Due to the influence of apoAI on the development of atherosclerosis, the focus of attention is now the identification of important structural and functional elements within the protein sequence.

ApoAI is initially synthesized as a preproapolipoprotein. The 18 amino acid prepeptide is cleaved as the apoAI is translocated across the membrane of the endoplasmic reticulum (Zannis et al., 1983; Folz & Gordon, 1987), and the 6 residue propeptide is subsequently removed in the plasma or lymph (Edelstein et al., 1983). Where studied, the properties of recombinant HDL assembled with proapoAI and h-apoAI are similar. The size of particles (Sorci-Thomas et al., 1996) and number of apoAI molecules per particle and their ability to promote efflux of cholesterol and phospholipid are the same (Sviridov et al., 1996; Westman et al., 1993). LCAT activation by recombinant discoidal complexes incorporating either proapoAI or plasma-derived apoAI is similar (Sorci-Thomas et al., 1996), and further data in this paper indicate the similarity in α-helical contents. The exact function of the pro-segment has yet to be elucidated.

In vitro expression of proteins has been extensively utilized to study their structure and function. We have previously developed an insect cell/baculovirus expression system (Pyle et al., 1995) for the expression of secreted proapoAI with yields of up to 80 mg/L. However, owing to its complexity, this system is not readily available for the rapid screening of protein mutants. For this latter process, we have looked to expression in *Escherichia coli*. In the present study,

† Supported by the National Health and Medical Research Council of Australia. Y.F. is supported by the Japan Foundation for Aging and Health.

* Address correspondence to this author at the Baker Medical Research Institute, P.O. Box 348, Prahran, Victoria 3181, Australia.
‡ Baker Medical Research Institute.
§ University of Melbourne.

⊗ Abstract published in *Advance ACS Abstracts,* August 15, 1996.

[1] Abbreviations: apoAI, apolipoprotein AI; DMPC, L-α-dimyristoylphosphatidylcholine; DMSO, dimethyl sulfoxide; DSP, dithiobis-(succinimidyl propionate); GST, glutathione *S*-transferase; h-apoAI, human apoAI; HDL, high-density lipoprotein; IPTG, isopropyl β-D-thiogalactoside; LCAT, lecithin:cholesterol acyltransferase; PBS, phosphate-buffered saline; PC, phosphatidylcholine; PCR, polymerase chain reaction; SDS−PAGE, sodium dodecyl sulfate−polyacrylamide gel electrophoresis; TLC, thin-layer chromatography.

S0006-2960(96)00907-5 CCC: $12.00

proapoAI was expressed intracellularly in fusion with glutathione *S*-transferase (GST) (Smith & Johnson, 1988) to facilitate recovery of protein by single-step affinity chromatography and allow for recovery of the apolipoprotein alone following thrombin cleavage of the fusion protein. Although apoAI has been expressed as a fusion protein in *E. coli* previously, yields of pure apoAI have been low after cleavage with factor Xa (Schmidt et al., 1995), or the protein has been partially truncated during synthesis (Brissette et al., 1991). This paper describes the production and characteristics of full-length and intentionally truncated versions of proapoAI using the *E. coli*/pGEX vector system, with yields of 5−20 mg/L. These truncation mutants were designed to further investigate particular regions of apoAI, previously identified by monoclonal antibodies, which appear to have some function related to cholesterol efflux (Sviridov et al., 1996).

The various recombinant forms of apoAI were investigated structurally by circular dichroism, iodide quenching, and fluorescence anisotropy. The ability of the proteins to self-associate was analyzed by cross-linking followed by sodium dodecyl sulfate−polyacrylamide gel electrophoresis (SDS−PAGE), and several forms were examined for their ability to activate LCAT.

MATERIALS AND METHODS

Materials. Full-length human apoAI cDNA was a gift from Dr. Shula Metzger, Hadasseh Hospital, Jerusalem, Israel, and the pGEX-KN vector was provided by Dr. Jack Dixon, Michigan. Glutathione−agarose, reduced glutathione, human thrombin, and aprotinin were purchased from Sigma. Dithiobis(succinimidyl propionate) (DSP) was from Pierce, 8−16% polyacrylamide gradient gels were from NOVEX, and 3−30% gels were from Gradipore; Microcon microconcentrators were obtained from Amicon. Taq DNA polymerase was from Perkin Elmer; 5′ and 3′ pGEX sequencing primers were from Pharmacia. The Sequenase II DNA sequencing kit was from USB, and all other oligonucleotides were purchased from Bresatec, Australia. [4-^{14}C]Cholesterol (specific activity 2.0 Gbq/mmol) was purchased from NEN−DuPont.

Construction of Recombinant Plasmids. Based on the method described by Hakes and Dixon (1992), full-length human apoAI cDNA was amplified by the polymerase chain reaction (PCR) using the following primers: 5′ primer, TTTGCGGCCGCCTGGTTCCGCGTCGGCATTTCTGGCAG; 3′ primer, TTTGAATTCTCACTGGGTGTTGAGC. The 5′ primer introduces a *Not*I site followed by a sequence coding for a thrombin cleavage site immediately preceding the sequence coding for the first five amino acids of the prosegment of apoAI. The 3′ primer introduces an *Eco*RI restriction site after the stop codon for protein translation. Truncated versions of proapoAI cDNA were prepared by using the same 5′ primer and similar 3′ primers designed to introduce a stop codon after the sequence of DNA coding for the newly selected carboxy-terminal amino acid. The chosen termination residues were amino acids 243 (full-length), 222, 210, 150, and 135. PCR products were ligated into the *Not*I/*Eco*RI sites of pGEX-KN, and the recombinant plasmid was transformed into the protease-deficient *E. coli* strain BL21(DE3). All plasmids from clones selected for expression of recombinant apoAI were subsequently sequenced.

Expression of Recombinant ApoAI in E. coli. Human proapoAI (full-length and truncated) was expressed according to Smith and Johnson (1988) and *GST, Gene Fusion System Manual* (1993), with modifications. *E. coli*, transformed with pGEX-KN/proapoAI constructs, was cultured in 2YT broth containing 50 μg/mL ampicillin and 2% (w/v) glucose until reaching an A_{600} of 0.9−1.0. Isopropyl β-D-thiogalactoside (IPTG) was added to a final concentration of 0.1 mM and incubation continued for a further 2.5 h. Cells were pelleted (7700*g*, 10 min), resuspended in phosphate-buffered saline (PBS) containing aprotinin (0.04 trypsin inhibitory unit/mL), and sonicated. Cell debris was removed by centrifugation (12000*g*, 10 min) and the soluble fraction loaded onto a glutathione−agarose column (1.5 × 7 cm). Fusion protein bound to the column was eluted via the addition of reduced glutathione (10 mM in 0.05 M Tris/HCl, pH 8.0), and to obtain apoAI free of the carrier GST, fusion protein was cleaved by the addition of approximately 0.7−1.8 NIH units of thrombin/mg of fusion protein at 25 °C for 16 h. The solution was dialyzed, and free proapoAI was separated from the GST carrier by repeating the affinity chromatography as described above.

Purification of Plasma ApoAI. Briefly, HDL_3 (d = 1.125−1.210 g/mL) was isolated by ultracentrifugation (Havel et al., 1955), washed by recentrifugation at the same density, and delipidated using chloroform, methanol, and ether as extracting solvents (Herbert et al., 1973). ApoAI was purified by gel filtration and ion-exchange chromatography as described before (Morrison et al., 1990).

Preparation of Egg Yolk Phosphatidylcholine Vesicles and Formation of Lipid−Protein Complexes. L-α-Phosphatidylcholine (PC) vesicles were prepared as previously described (Sviridov & Fidge, 1995). The unilamellar vesicles were used to test the lipid binding properties of expressed proapoAI which was incubated with the PC at a protein: lipid (w/w) ratio of 1:4 or greater, in PBS for 3 h at 37 °C (Morrison et al., 1991).

Analytical Methods. Protein concentrations were measured according to the Bradford method (Bradford, 1976) using bovine serum albumin as standard.

LCAT Assay. LCAT was isolated from fresh human serum by a sequence of ultracentrifugation, phenyl-sepharose, ion-exchange (DEAE-Sephacel), and hydroxylapatite chromatography as described previously (McLean et al., 1986). To assess the activity of apoAI as a cofactor, varying concentrations of apoprotein were preincubated for 1 h at 37 °C with a constant concentration of substrate, comprising single-bilayer vesicles of PC (25 μg), cholesterol (0.75 μg), and [^{14}C]cholesterol (0.5 μg, final radioactivity 6 × 10^5 dpm/mL), prepared as described previously (Zorich et al., 1985) with minor modifications. The reaction, in a total volume of 0.25 mL, was initiated by the addition of purified LCAT (0.1 μg), and after 60 min at 37 °C, the lipids were extracted, and the cholesteryl ester fraction was obtained by TLC and quantitated by scraping and liquid scintillation counting (Skipsi & Barclay, 1969). Under these conditions, less than 5% of [^{14}C]cholesterol was converted to cholesteryl ester.

Cross-Linking of Proteins. Proteins equilibrated in PBS were mixed in solution with a 2−60-fold molar excess of DSP dissolved in dimethyl sulfoxide (DMSO) such that the final concentration of DMSO did not exceed 10% of volume. Samples were incubated for 30 min at room temperature, and then quenched with 50 mM Tris/HCl, pH 7.3, for 15

min. Samples volumes were reduced for electrophoresis using Microcon microconcentrators.

Polyacrylamide Gel Electrophoresis, Immunoblotting. Protein samples were separated by electrophoresis on 12 or 15% polyacrylamide gels containing 0.1% SDS. Cross-linked proteins were separated on 8−16% polyacrylamide gradient gels. Either proteins were stained with Coomassie Brilliant Blue and the cross-linked proteins analyzed by densitometry using an LKB Ultrascan XL laser densitometer, or proteins were transferred to nitrocellulose by electroblotting. Western blotting was performed using a monospecific rabbit antiserum to h-apoAI, and then anti-rabbit IgG coupled to horseradish peroxidase (second antibody) to allow color development as described previously (Allan et al., 1993).

Isoelectric Focusing (IEF). IEF was performed in a Mini Protean II electrophoresis chamber (Bio-Rad) on 8 cm × 7 cm 7.5% polyacrylamide slab gels (1.5 mm). Gel solutions contained 8 M deionized urea (Promega) and 5% (v/v) ampholine (pH 4−6.5: Pharmacia−LKB). Gels were pre-focused for 30 min at 100 V; protein samples were loaded and focused at 200 V for 30 min and then at 300 V for 2 h. The pH gradient was determined by cutting a small portion of blank gel into 3 mm slices, equilibrating each slice in 0.75 mL of deionized water for 30 min, and measuring the pH of the resulting solution.

Peptide Methods. Automated amino acid sequence analysis was performed using an Applied Biosystems Model 470A sequence equipped with an on-line Model 120A PTH analyzer (Applied Biosystems). The molecular mass of expressed proapoAI forms was determined by ion spray mass spectrophotometric analysis performed by Chiron Mimotropes Peptide Systems, Clayton, Victoria.

Physical Chemistry. (A) Preparation of Samples. All samples were prepared in 20 mM sodium phosphate buffer, pH 7.2. Unilamellar phospholipid vesicles of L-α-dimyristoylphosphatidylcholine (DMPC) were prepared by sonication (MSE Soniprep) under nitrogen according to standard procedures (Woodle & Papahadjopoulas, 1989). Suspensions were centrifuged at 436000*g* for 1 h to remove any titanium fragments. Protein−DMPC complexes were prepared by incubating protein with DMPC vesicles (1:3.4 w/w) at 37 °C for 1 h. To examine the amount of free protein, complexes were subjected to native polyacrylamide gel electrophoresis on 3−30% gradient gels, run at 50 V for 16 h, and free protein was quantitated by densitometry of stained gels.

(B) Circular Dichroism. Measurements were made with an Aviv Model 62DS spectrometer at 27 °C in a 0.5 mm path length cuvette, at protein concentrations of 0.2 mg/mL in 20 mM phosphate buffer, pH 7.2. Data were collected from 185 to 250 nm at 0.5 nm intervals. Data obtained for protein−DMPC complexes were corrected by subtraction of a base line obtained for vesicles alone. CD spectra were fitted between 190 and 240 nm according to the method of Yang et al. (1986) to obtain percentages of α-helices.

(C) Fluorescence Experiments. Fluorescence measurements were made with a Perkin Elmer LS-5 spectrofluorometer thermostated at 27 °C. Quenching experiments were performed by the addition of aliquots of a stock solution of KI (5 M containing trace amounts of $Na_2S_2O_3$ to prevent the formation of I_3). The accessibility of tryptophan residues was determined from the ordinate intercept of a secondary plot of $F_o/\Delta F$ versus 1/[quencher], where F_o is the fluorescence intensity in the absence of quencher and ΔF is the reduction in fluorescence due to the quencher (Lehrer, 1971). For quenching and anisotropy experiments, the excitation and emission wavelengths were 280 and 334 nm, respectively. The anisotropy (r) was calculated according to $r = (I_v - GI_H)/(I_V + 2GI_H)$, where G is the grating correction factor and I_V and I_H are the intensities of the vertically and horizontally polarized components of the emission, respectively.

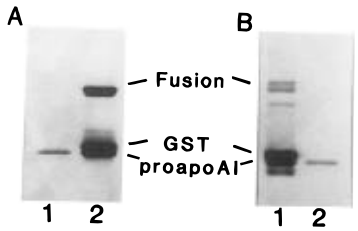

FIGURE 1: ProapoAI degradation by double digestion with thrombin. Proteins were detected by Coomassie Brilliant Blue staining after 12% SDS−PAGE. (A) GST/proapoAI fusion protein digested overnight at room temperature with thrombin, 0.8 NIH unit/mg (Sigma) of fusion protein. Lane 1, h-apoAI; lane 2, incompletely cleaved GST/proapoAI. (B) Further digestion of the partially cleaved product with thrombin, 0.13 NIH unit/mg of fusion protein. Lane 1, cleaved fusion protein: lane 2, h-apoAI.

RESULTS

Production of ProapoAI by E. coli. SDS−PAGE analysis of the *E. coli* expressed protein, purified by glutathione−agarose affinity chromatography, revealed an expected (approximately) 55 kDa GST/proapoAI fusion product (data not shown). Initial attempts to cleave the fusion product while it was still bound to the column resulted in the appearance of an unexpected band, a few kilodaltons smaller than an h-apoAI control on SDS−PAGE, and so this method of cleavage was not pursued (data not shown). Cleavage was therefore performed after column elution to yield a band migrating similarly to h-apoAI (approximately 29 kDa) observed by SDS−PAGE, (see Figure 1). It was initially observed that if cleavage of the fusion product was incomplete after a single digestion, supplementation with additional thrombin resulted in some proteolysis of the cleaved proapoAI generating a lower molecular weight protein as shown in Figure 1. It was essential, therefore, to remove free proapoAI before further digestion (if required) was performed. Western blotting showed that the purified 29 kDa protein was immunologically identical to apoAI, and the p*I* of the recombinant proapoAI according to IEF was consistent with it being 2 charge units more basic than mature apoAI (data not shown). N-Terminal sequencing confirmed the expected proapoAI sequence. Cleavage of the truncated forms of GST/proapoAI did result in some degradation of the proapoAI proteins. Utilizing Sigma Gel to scan SDS−PAGE gels of purified proteins, this was determined to be less than 7% for proapoAI$_{-6-243}$ and proapoAI$_{-6-135}$ and ranging between 1.2 and 9.2% for proapoAI$_{-6-150}$ and 2.8−9.6% for proapoAI$_{-6-222}$. For proapoAI$_{-6-210}$, more heterogeneity in size was observed in that apart from significantly smaller degradation products present as 8.0% of the total protein, the major protein band could be seen to contain a slightly smaller product not detectable as a separate species by the Sigma Gel analysis. SDS−PAGE of all proapoAI forms is shown in Figure 2.

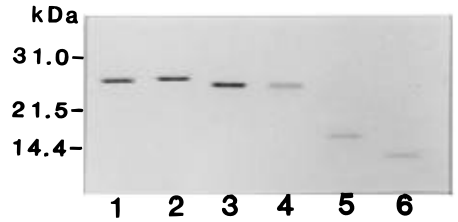

FIGURE 2: Full-length and truncated proapoAI. Proteins were detected by Coomassie Brilliant Blue staining after 15% SDS−PAGE. Lane 1, h-apoAI; lane 2, proapoAI$_{-6-243}$; lane 3, proapoAI$_{-6-222}$; lane 4, proapoAI$_{-6-210}$; lane 5, proapoAI$_{-6-150}$; lane 6, proapoAI$_{-6-135}$.

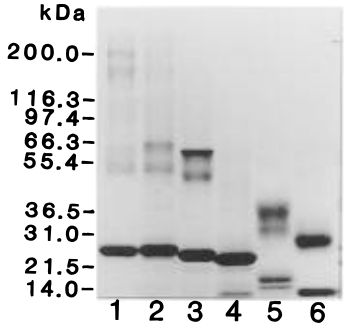

FIGURE 3: Self-association of full-length and truncated proapoAI. All proteins (35.3 μM) were cross-linked with 200 μM DSP as described under Materials and Methods and separated by 8−16% SDS−PAGE, and the bands were detected with Coomassie Brilliant Blue. Lane 1, h-apoAI; lane 2, proapoAI$_{-6-243}$; lane 3, proapoAI$_{-6-222}$; lane 4, proapoAI$_{-6-210}$; lane 5, proapoAI$_{-6-150}$; lane 6, proapoAI$_{-6-135}$.

The sizes of full-length and truncated forms of proapoAI were established by ion spray mass spectrophotometric analysis and yielded the following molecular masses: full-length proapoAI$_{-6-243}$, 28 963 Da; proapoAI$_{-6-222}$, 26 517 Da; proapoAI$_{-6-210}$, 25 170 Da; proapoAI$_{-6-150}$, 18 527 Da; and proapoAI$_{-6-135}$, 16 771 Da. The calculated molecular masses were almost identical to their theoretical molecular masses, the largest estimated difference being less than 3 Da. The yield of apoAI and truncated forms varied between 5 and 20 mg/L, with some batch to batch variation of the same form being observed.

Binding of Recombinant Full-Length ProapoAI to Lipid. To establish that the expressed full-length proapoAI met the essential criterion for its classification as an apolipoprotein, namely, its ability to bind lipid, proapoAI was incubated with egg yolk PC unilamellar vesicles (see Materials and Methods) for 3 h at 37 °C. After ultracentrifugation, greater than 90% of the proapoAI was recovered in the top $d < 1.25$ g/mL fraction, demonstrating that the expressed proapoAI does bind lipid (data not shown).

Self-Association of Recombinant ProapoAI Forms. It is known that apoAI undergoes concentration-dependent self-association. To assess the ability of the expressed proapoAI forms to self-associate, samples were incubated at concentrations of 3.5−88 μM in PBS and cross-linked with DSP. Whereas the h-apoAI control showed a concentration-dependent self-association with formation of high molecular weight oligomers, the recombinant full-length proapoAI seldom formed oligomers larger than a trimer (Figure 3). Similarly, the largest self-associated form of proapoAI$_{-6-222}$ was a trimer, while proapoAI$_{-6-210}$ did not appear to self-associate at all (Figure 3); a small amount of apparently

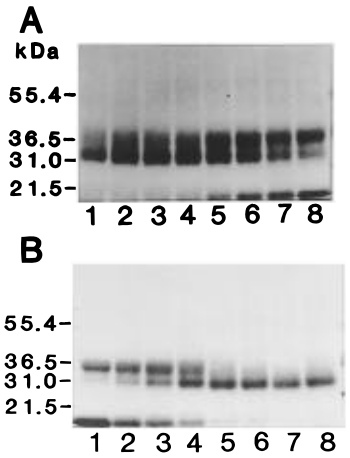

FIGURE 4: Effect of cross-linker concentration on self-association of proapoAI$_{-6-150}$. Cross-linked proteins were separated by 8−16% SDS−PAGE and the bands detected by Coomassie Brilliant Blue staining. (A) ProapoAI$_{-6-150}$ at the concentrations indicated below was cross-linked with 200 μM DSP as described under Materials and Methods. (B) ProapoAI$_{-6-150}$ cross-linked with a 10-fold molar excess of DSP. Lane 1, 3.5 μM; lane 2, 7.0 μM; lane 3, 10.6 μM; lane 4, 17.6 μM; lane 5, 35.3 μM; lane 6, 53.0 μM; lane 7, 70.6 μM; lane 8, 88.0 μM.

degraded protein for proapoAI$_{-6-210}$ and proapoAI$_{-6-150}$ is observable in these preparations. The degree of self-associated proapoAI$_{-6-150}$ appeared to depend on the DSP:protein ratio. At higher DSP:protein molar ratios, mostly dimers were formed, whereas trimeric forms dominated as the DSP:protein ratio was reduced. To illustrate this point, when increasing concentrations of protein were incubated with a constant 10-fold molar excess of DSP, trimers dominated at low concentrations of protein, whereas dimers formed at high concentrations of protein (Figure 4A). In contrast, when DSP concentration was kept constant and protein concentration increased such that the DSP:protein molar ratio decreased, trimers became the main species, and the formation of dimers decreased (Figure 4B). This result suggests that the protein:cross-linker concentration is an important factor in self-association and apparently the hydrophobic DSP is somehow disrupting trimer formation in favor of dimers as the concentration of cross-linker increases. The smallest protein proapoAI$_{-6-135}$ formed only dimers. At a proapoAI$_{-6-135}$ concentration of 88 μM with DSP at 880 μM, dimers constituted over 80% of the protein as determined by densitometry.

Secondary Structure of Recombinant ProapoAI Forms Assessed by Circular Dichroism. The results of circular dichroism experiments are summarized in Table 1. Free in solution, the helix content of h-apoAI was 43%, increasing to 69% when associated with DMPC. A smaller increase was noted when egg phosphatidylcholine was the host lipid (data not shown). The helix content of expressed proapoAI$_{-6-243}$ was 51%, which increased to 65% when associated with DMPC. It should be noted that when proapoAI$_{-6-243}$ was denatured and renatured the α-helix value for the free protein dropped to 45%, which was very close to the 43% of similarly treated h-apoAI. The helix content of the lipid-associated forms of these proteins is comparable even when recombinant proapoAI is left untreated. The results from the gradient gel electrophoresis followed by densitometry, used to assess quantities of free protein after DMPC binding, indicated that for h-apoAI and

Table 1: Percent α-Helix in Recombinant Full-Length ProapoAI and Truncated Forms Determined by Circular Dichroism Spectroscopy

species	in solution	in DMPC complex[a]	theoretical[b]
proapoAI$_{-6-135}$	39	52	57
proapoAI$_{-6-150}$	39	58	60
proapoAI$_{-6-210}$	44	58	69
proapoAI$_{-6-222}$	45	54	66
proapoAI$_{-6-243}$	51	65	69
proapoAI$_{-6-243}$[c]	45	66	69
h-apoAI	43	69	69

[a] Protein was incubated with DMPC vesicles (1:3.4 w/w) at 37 °C for 1 h. [b] Theoretical content of α-helix based on sequence analysis (Boguski et al., 1986). [c] After extraction with organic solvents and denaturation in 6 M urea as per h-apoAI; see *Purification of Plasma ApoAI* under Materials and Methods.

Table 2: Anisotropy of Tryptophan Residues in Recombinant Forms of ProapoAI and Their Fractional Accessibility to Quenching by Iodide

	accessibility (±0.02)		anisotropy (±0.002)	
species	in solution	in DMPC complex[a]	in solution	in DMPC complex[a]
proapoAI$_{-6-135}$	0.97	1.0	0.087	0.065
proapoAI$_{-6-150}$	0.86	1.00	0.080	0.070
proapoAI$_{-6-210}$	0.73	0.83	0.081	0.076
proapoAI$_{-6-222}$	0.50	1.0	0.084	0.077
proapoAI$_{-6-243}$	0.42	0.54	0.084	0.068
proapoAI$_{-6-243}$[b]	0.72	*nd*[c]	0.099	*nd*
h-apoAI[b]	0.73	0.80	0.092	0.062

[a] Protein was incubated with DMPC vesicles (1:3.4 w/w) at 37 °C for 1 h. [b] After extraction with organic solvents and denaturation in 6 M urea as per h-apoAI; see *Purification of Plasma ApoAI* under Materials and Methods. [c] *nd*, not done.

proapoAI$_{-6-243}$ lipid-free protein was not present. This was also observed for the truncated forms proapoAI$_{-6-135}$ and proapoAI$_{-6-150}$. However, the forms proapoAI$_{-6-210}$ and proapoAI$_{-6-222}$ yielded 9.5% and 12.8% uncomplexed protein, respectively. Taking this into account, the helix content of the truncated proapoAI forms in solution varied from 39% to 45%, roughly increasing as the length of the protein approached that of the full-length form. When complexed with DMPC, the sequence between residues 150 and 222 does not contribute to the helicity of the protein, which seems to indicate that the C-terminal region of the protein is required for the formation of helix between residues 150 and 222. Table 2 also lists the theoretical content of α-helix of each form based on the model of Boguski et al. (1986). There is reasonable agreement between experimental and theoretical values for proapoAI$_{-6-135}$, proapoAI$_{-6-150}$, proapoAI$_{-6-243}$, and h-apoAI, but the lower helix values for proapoAI$_{-6-210}$ and proapoAI$_{-6-222}$ are again evident. Interestingly, position 192 is very susceptible to proteolytic cleavage (Ji & Jonas, 1995), and the recombinant protein proapoAI$_{-6-210}$ seems vulnerable to nonspecific thrombin digestion, suggesting that a relatively open structure exists in this region of the protein sequence.

We note that the helical content of proapoAI$_{-6-222}$ (45% in solution and 54% in the DMPC complex) is comparable to values for apoAI$_1$−192 reported by Ji and Jonas (1995) (52% in solution and 57−58% complexed to palmitoyloleoylphosphatidylcholine), and for apoAI$_{1-189}$ (Δ190−243) reported by Holvoet et al. (1995) (52% complexed to dipalmitoylphosphatidylcholine). Some of these differences result from differences in the host phospholipid.

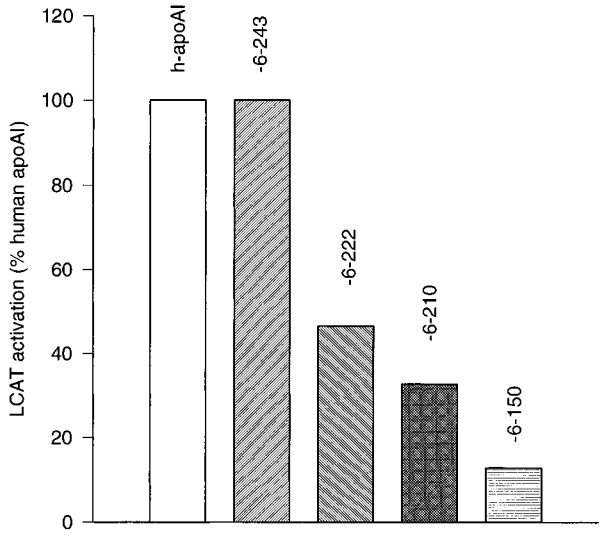

FIGURE 5: Activation of LCAT by different forms of proapoAI. Data are presented as the percent activation relative to h-apoAI for which 100% corresponds to the activity of 264 pmol of cholesteryl ester (0.1 μg of LCAT)$^{-1}$ h^{-1}. Less than 5% of [^{14}C]cholesterol was converted to cholesteryl ester.

Accessibility and Anisotropy of Tryptophan Residues. The accessibility of the tryptophans in the recombinant forms is summarized in Table 2 together with the anisotropy of the tryptophan fluorescence. The five tryptophan residues of h-apoAI are located at positions −3, 8, 50, 72, and 107, and are therefore present in all of the truncated mutants. These residues are more than 86% accessible in proapoAI$_{-6-135}$ and proapoAI$_{-6-150}$, whether in free solution or complexed with DMPC. The presence of the C-terminal region of the molecule, particularly the region 223−243, reduces the accessibility by about 50% for both the solution and the complexed forms of the pro-protein. However this difference is reduced for the uncomplexed protein when the proapoAI$_{-6-243}$ is denatured and renatured prior to analysis. The presence of the C-terminal domain therefore appears to affect the structure of the N-terminal region of the molecule. Interestingly, proapoAI$_{-6-222}$ displays about 50% less accessibility when free than when complexed.

The tryptophan anisotropy (Table 2) is lower in the complex than in free solution, a result that has been observed previously for h-apoAI (Jonas et al., 1990). However, an increase in the quantum yield on association with DMPC by a factor of 1.14 for proapoAI$_{-6-135}$ to 1.49 for proapoAI$_{-6-243}$ suggests that this may be due, at least partially, to an increase in the fluorescence lifetime.

LCAT Activation by ProapoAI and Truncated Forms. As shown in Figure 5, the recombinant proapoAI was shown to activate highly purified LCAT to the same degree as h-apoAI, while several truncated forms showed a marked reduction in LCAT activation.

DISCUSSION

The structural domains of apoAI that determine its physiological function(s) have not been identified with certainty, although recent evidence would suggest that specific sites determine important biochemical events. Our laboratory has identified a carboxy-terminal region of apoAI

which recognizes cellular HDL binding proteins (Allan et al., 1993) a finding supported by Dalton and Swaney (1993). Certain unique epitopes of apoAI may influence the ability of HDL to promote cholesterol efflux from cells (Banka et al., 1994; Fielding et al., 1994; Sviridov et al., 1996), and specific regions of apoAI have also been implicated in the activation of LCAT [see review by Fielding and Fielding (1995)].

The expression of apoAI and apoAI mutants, engineered to identify active regions of the protein, has been addressed by several laboratories, but many investigations have been hampered by low yields of apoAI obtained from expression systems [see Brouillette and Anantharamaiah (1995)]. In one case, the expression of carboxy-terminally deleted apoAI gave yields varying from 0.1 to 10 μg/mL (Schmidt et al., 1995).

In the present study, we focused attention on the production of several truncated versions and the full-length proapoAI. Data on the properties of these mutants should provide helpful information on the several candidate regions of apoAI that mediate cholesterol efflux, lipid binding, cell receptor interaction, or LCAT activation. The recombinant full-length proapoAI was assessed by ion spray mass spectrometry to have the correct molecular weight, had immunoreactivity similar to h-apoAI by Western blot, and was able to activate LCAT to the same extent as h-apoAI. The structural validity of the truncated forms of proapoAI was also analyzed by ion spray mass electrophoretic analysis, which confirmed with remarkable precision the expected molecular weight of each protein.

The availability of mutated forms of apoAI enabled us to explore the secondary structure of apoAI and to follow structural changes induced by interaction of the various forms with lipid. From both circular dichroism and tryptophan fluorescent experiments, the carboxy-terminal portion of apoAI emerged as an important contributor to the secondary structure of this apoprotein. Specifically, the circular dichroism results indicate that between the region 150−222 no additional helicity is gained until the C-terminal sequence 222−243 is present in the molecule. Moreover, the iodide quenching results indicate that the accessibility of tryptophan residues characteristic of the full-length forms is not attained until the C-terminal sequence 222−243 is present. These results suggest that the strictly antiparallel arrangement of the amphipathic-helical repeat units is not attained until the full-length sequence is present. One possibility is that residues in the region 150−222 hinge away from the lipid surface and do not adopt a helical conformation around the edge of the apoAI−DMPC complex until the C-terminal domain is present. Indeed, molecular modeling has suggested that charge complementarity between adjacent helices is a requirement for stable interaction with the lipid as well as amphipathicity of the helix itself (Lins et al., 1995).

The production of these mutants was also useful for probing the self-association properties of apoAI, a phenomenon which although observed by many investigators over several years has not been distinctly connected with any physiological function. Although we obtained high molecular weight oligomers from native apoAI, surprisingly with recombinant proapoAI self-association did not progress strongly past the trimeric stage, indicating that the residues forming the prosequence compromise the regions involved in self-association. Truncation of 21 C-terminal residues completely arrested oligomer formation to the trimeric stage, while removal of 33 residues (proapoAI$_{-6-210}$) arrested self-association almost completely. This latter result is not completely clear, however, because of the heterogeneity of the expressed product. The shorter form proapoAI$_{-6-150}$ was able to form trimers, although the present studies have demonstrated that cross-linker concentration can affect the result. Further truncation to 135 clearly terminated self-association at the dimeric level. Overall, the studies are in agreement with the findings of Ji and Jonas (1995) that the C-terminus contributes to the self-association of apoAI, although in our experiments, we have also shown that further deletion of the C-terminal residues restores some of the self-association properties of proapoAI. Possibly, the C-terminus previously masked the potential protein−protein interaction property of the central domain. It is not possible to distinguish between the participation of secondary structure (α-helices) from that of specific sequences in self-association from these studies, but they suggest that deletion of specific central regions should also be explored for this purpose.

While full-length recombinant proapoAI activates LCAT to the same degree as human plasma-derived apoAI, the truncated forms show markedly less activation. Initial data indicate that deletion of only a few carboxy-terminal residues (recombinant apoAI$_{-6-222}$) reduces the ability of proapoAI to activate LCAT by approximately 53% and the activity is sequentially reduced by further deletion as shown in Figure 5. The data for proapoAI$_{-6-210}$ of approximately 33% are somewhat higher than the result obtained by Minnich et al. (1992), who showed that truncation to residue 212 (Δ213−243) severely reduced LCAT activation to 13% of the intact apoAI, although their methodology was slightly different. Uncertainty persists as to the precise region of apoAI involved, but as recently reviewed by Fielding and Fielding (1995), residues 98−143 seem to be necessary for LCAT activation. Ji and Jonas (1995) suggest that the decreased LCAT activity reported by other groups for deletion mutants but not for their truncated form apoAI$_{1-192}$ relates to incomplete lipid binding and failure to isolate pure particles. The importance of this suggestion, also supported by Holvoet et al. (1995), is that the conformation of apoAI within recombinant HDL has a major effect on LCAT activation. Further work is needed to unravel the complexity of the apoAI−LCAT association.

In conclusion, we have established a system for the production of recombinant proapoAI and mutated forms enabling a more detailed examination of the structure/function relationship of apoAI.

ACKNOWLEDGMENT

We thank Robert Chan for excellent technical assistance.

REFERENCES

Allan, C. M., Fidge, N. H., Morrison, J. R., & Kanellos, J. (1993) *Biochem. J. 290*, 449−455.
Banka, C. L., Black, A. S., & Curtiss, L. K. (1994) *J. Biol. Chem. 269*, 10288−10297.
Barter, P. (1993) *Curr. Opin. Lipidol. 4*, 210−217.
Boguski, M. S., Freeman, M., Elshourbagy, N. A., Taylor, J. M., & Gordon, J. L. (1986) *J. Lipid Res. 27*, 1011−1034.
Bradford, M. M. (1976) *Anal. Biochem. 72*, 248−256.
Brissette, L., Cahuzac-Bec, N., Desforges, M., Bec, J.-L., Marcel, Y. L., & Rassart, E. (1991) *Protein Expression Purif. 2*, 296−303.

Brouillette, C. G., & Anantharamaiah, G. M. (1995) *Biochim. Biophys. Acta 1256*, 103−129.
Dalton, M. B., & Swaney, J. B. (1993) *J. Biol. Chem. 268*, 19274−19283.
Edelstein, C., Gordon, J. I., Toscas, K., Sims, H. F., Strauss, A. W., & Scanu, A. M. (1983) *J. Biol. Chem. 258*, 11430−11433.
Fielding, C. J., & Fielding, P. E. (1995) *J. Lipid Res. 36*, 211−228.
Fielding, C. J., Shore, V. G., & Fielding, P. E. (1972) *Biochem. Biophys. Res. Commun. 46*, 1493−1498.
Fielding, P. E., Kawano, M., Catapano, A. L., Zoppo, A., Marcovina, S., & Fielding, C. J. (1994) *Biochemistry 33*, 6981−6985.
Folz, R. J., & Gordon, J. I. (1987) *J. Biol. Chem. 262*, 17221−17230.
GST, Gene Fusion System Manual (1993) Pharmacia Biotechnology, pp 1−36.
Hakes, D. J., & Dixon, J. E. (1992) *Anal. Biochem. 202*, 293−298.
Havel, R. J., Eder, H. A., & Bragdon, J. H. (1955) *J. Clin. Invest. 34*, 1345−1353.
Herbert, P. N., Shulman, R. S., Levy, R. I., & Fredrickson, D. S. (1973) *J. Biol. Chem. 248*, 4941−4946.
Holvoet, P., Zhao, Z., Vanloo, B., Vos, R., Deridder, E., Dhoest, A., Taveirne, J., Brouwers, E., Demarsin, E., Engelborghs, Y., Rosseneu, M., Collen, D., & Brasseur, R. (1995) *Biochemistry 34*, 13334−13342.
Ji, Y., & Jonas, A. (1995) *J. Biol. Chem. 270*, 11290−11297.
Jonas, A. (1987) in *Plasma Lipoproteins* (Gotto, A. M., Jr., Ed.) p 299, Elsevier, Amsterdam.
Jonas, A., Wald, H., Toohill, K. L. H., Krul, E. S., & Kezdy, K. E. (1990) *J. Biol. Chem. 265*, 22123−22129.
Lehrer, S. (1971) *Biochemistry 10*, 33255−33262.
Lins, L., Brasseur, R., DePauw, M., Van Biervliet, J. P., Ruysschaert, J.-M., Rosseneu, M., & Vanloo, B. (1995) *Biochim. Biophys. Acta 1258*, 10−18.
Maciejko, J. T., Holmes, D. R., Kottke, B. A., Zinmeister, A. R., Dinh, D. M., & Mao, S. J. T. (1983) *N. Engl. J. Med. 309*, 385−389.
McLean, J., Fielding, C., Drayna, D., Dieplinger, H., Baer, B., Kohr, W., Henzel, W., & Lawn, R. (1986) *Proc. Natl. Acad. Sci. U.S.A. 83*, 2335−2339.
Minnich, A., Collet, X., Roghani, A., Cladaras, C., Hamilton, R. L., Fielding, C. J., & Zannis, V. I. (1992) *J. Biol. Chem. 267*, 16553−16560.
Morrison, J. R., Fidge, N. H., & Grego, B. (1990) *Anal. Biochem. 186*, 145−152.
Morrison, J. R., Fidge, N. H., & Tozuka, M. (1991) *J. Biol. Chem. 266*, 18780−18785.
Pyle, L. E., Barton, P., Fujiwara, Y., Mitchell, A., & Fidge, N. H. (1995*) J. Lipid Res. 36*, 2355−2361.
Schmidt, H. H.-J., Remaley, A. T., Stonik, J. A., Ronan, R., Wellmann, A., Thomas, F., Zech, L. A., Brewer B., & Hoeg J. M. (1995) *J. Biol. Chem. 270*, 5469−5475.
Skipsi, V. P., & Barclay, M. (1969). *Methods Enzymol. 14*, 30−598.
Smith, D. B., & Johnson, K. S. (1988) *Gene 67*, 31−40.
Sorci-Thomas, M., Kearns, M. W., & Lee, J. P. (1993) *J. Biol. Chem. 268*, 21403−21409.
Sorci-Thomas, M. G., Parks, J. S., Kearns, M. W., Pate, G. N., Zhang, C., & Thomas, M. J. (1996) *J. Lipid Res. 37*, 673−683.
Sviridov, D., & Fidge, N. (1995) *Biochim. Biophys. Acta 1256*, 210−220.
Sviridov, D., Pyle, L., & Fidge, N. (1996) *Biochemistry 35*, 189−196.
Westman, J., Roobol, C., Heymans, C., Carlson, L. A., & Wulfert, E. (1993) *Scand. J. Clin. Lab. Invest. 53*, 773−782.
Woodle, M. C., & Papahadjopoulas, D. (1989) *Methods Enzymol. 171*, 193−217.
Yang, J. T., Wu, C.-S. C., & Martinez, H. M. (1986) *Methods Enzymol. 130*, 228.
Zannis,V. I., Karathanasis, S. K., Keutmann, H. T., Goldberger, G., & Breslow, J. L. (1983) *Proc. Natl. Acad. Sci. U.S.A. 80*, 2574−2578.
Zorich, N., Jonas, A., & Pownall, H. J. (1985) *J. Biol. Chem. 260*, 8831−8837.

BI9609073